

# A Design Concept of a Multi-Chambered Radial In-Flow (MCRI) Bipropellant Rocket Engine

Ben Glass

under the direction of  
Col. John E. Keesee  
Massachusetts Institute of Technology

Research Science Institute  
August 1, 2002

## **Abstract**

A Multi-Chambered Radial In-flow (MCRI) Engine is a new type of annular rocket engine that has the potential for lower engine weight and higher performance at all altitudes. The MCRI concept uses a continuously self-optimizing, externally constrained expansion nozzle, capable of producing optimal thrust levels at any altitude, coupled with the ability to perform differential throttling for the purpose of thrust vectoring. This paper describes the design of the initial MCRI test engine and discusses the future testing of this new engine concept.

# 1 Introduction

A Multi-Chambered Radial In-Flow (MCRI) engine is a type of annular rocket engine. An annular engine is a rocket engine in which the expanding exhaust gasses in the nozzle are not constrained by permanent walls on all sides, but rather, either the inside or outside nozzle wall is formed by the surrounding ambient pressure[1]. Annular rocket engines are advantageous because they are continuously self-optimizing for operation at any altitude or in a vacuum condition. In Figure 1, a comparison of a conventional engine and a toroidal chambered radial in-flow engine are given. As can be seen, the radial in-flow engine does not have a set nozzle exit, which is what allows the engine to continuously self-optimize.

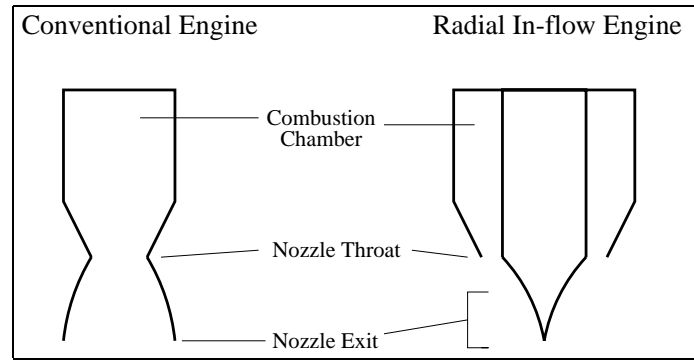


Figure 1: Section Views of a Conventionsl Engine and a Radial In-flow Engine

In an MCRI engine, the combustion chamber is similar to the toroidal chamber found in regular radial in-flow engines, with the key difference that in the MCRI engine, the main torus is divided into three or more sub-chambers. Each sub-chamber is isolated from the others by a dividing wall and seperate feed system, allowing each sub-chamber to operate at a performance level independent of the other sub-chambers. As will be discussed in section 3.6, this system enables two-dimensional thrust-vectoring that would otherwise require complex and heavy gimballing mechanisms.

A fully developed MCRI engine would provide performance advantages throughout all

altitudes, as well as reduced weight compared with conventional thrust vectoring techniques. MCRI engines will be utilized in applications which currently suffer from the lack of propulsion systems that demonstrate both high performance over a large altitude range and thrust vectoring capabilities. Examples of such applications include reusable space launch vehicles that require maneuverability for reentry and inter-continental ballistic missiles (ICBM's).

## 2 History

The basic idea behind annular and other externally-constrained rocket engines has been around for well over 40 years. There are even claims that German engineers tried to build an annular engine during WWII. In the U.S., annular engines were first developed by Rocketdyne, then a division of Rockwell Aerospace, during the 1960s. Rocketdyne tested many different annular engines, as large as 250,000-pound-thrust, and their original proposal for the Space Shuttle Main Engine was based on a radial in-flow type design [2].

During the 1970s and 1980s, very little progress was made into the development of externally constrained rocket engines. However, during the 1990s, Rocketdyne developed two linear aerospoke engines, the RS-2200 and XRS-2200, for use in the X-33 and VentureStar programs, respectively. Both of these engines have multiple combustion chambers lined up along two linear inner nozzle walls, called *ramps*. Although they show many of the advantages proposed by the MCRI engine they can be utilized in relatively few applications because of their rectangular shape.

There has been very little development of multi-chambered or clustered radial in-flow engines, and nearly no hot-fire test information.

## 3 Design Considerations

The design goal of the MCRI test engine is to prove the concept and feasibility of a multi-chambered radial in-flow engine capable of *differential throttling*, or individually throttling each sub-chamber, for the purpose of *thrust vectoring*, or changing the direction vector of the rocket’s useful thrust. The idea uses and adds to two previously proven technologies: Radial In-flow engines and engine throttling. Once the test engine is built and tested, the concept will be further refined and developed. The initial test engine will be kept small in order to accommodate the provided facilities and to maintain a low overhead. This section discusses the design of the initial test engine.

### 3.1 Basic Parameters

#### 3.1.1 Propellants

Cooling system design is particularly difficult for radial in-flow engines (see section 3.4). Considering this, gaseous oxygen (GOX) and gaseous hydrogen (GH<sub>2</sub>), which produce a low flame temperature, will be used as the oxidizer and fuel, respectively, for the MCRI test engine. In addition, these propellants also offer very high performance values. In table 1, GOX and GH<sub>2</sub> are compared with two common propellant combinations<sup>1</sup> [1].

Oxidizer	Fuel	O/F	$I_{sp}$ (sec)	$T_c$ (°R)	$C^*$ (ft./sec)
GOX	GH <sub>2</sub>	4	390	5374	7836
LOX	RP-1	2.5	300	6617	5902
F <sub>2</sub>	H <sub>2</sub>	8	410	7132	8385

Table 1: Performance Values of Common Rocket Propellants

O/F is the ratio of oxidizer mass to fuel mass,  $I_{sp}$  (specific impulse) is the amount of

---

<sup>1</sup>Values in Table 1 are given for a chamber pressure of 1000 *psia*

thrust a given propellant combination produces per pound of propellant burned,  $T_c$  is the chamber temperature and  $C^*$  is the characteristic exhaust velocity.

### 3.1.2 Thrust

Thrust ( $F$ ) is a measure of the effective force produced by a rocket engine. The MCRI test engine will be small, with a thrust of 250 lbs. Thrust is given by the following equations

$$F = \dot{M}V_e + (P_e - P_a)A_e \quad (1)$$

where  $\dot{M}$  is the total propellant mass flow (*slugs/sec*),  $V_e$  is the velocity at the nozzle exit (*ft/sec*),  $P_e$  is the nozzle exit pressure (*psia*),  $P_a$  is the atmospheric pressure (*psia*) and  $A_e$  is the nozzle exit area (*in<sup>2</sup>*). As seen in Equation (1), a rocket engine produces two types of thrust:  $\dot{M}V_e$  gives the momentum thrust, which is equal to the momentum of the ejected exhaust gasses while  $(P_a - P_e)A_e$  gives the pressure thrust and is equal to the product of the nozzle exit area and the pressure difference between the ambient atmosphere and the nozzle exit pressure. A rocket nozzle produces the most thrust and is said to be at its *optimal expansion ratio* when  $P_e = P_a$ . However, this condition exists at only one altitude for a given bell nozzle shape. At lower altitudes, the pressure thrust is negative and counterproductive, while at higher altitudes, incomplete expansion lowers the  $V_e$  term. In an annular nozzle the effective nozzle shape changes along with  $P_a$  and the nozzle operates at its optimal expansion ratio, regardless of altitude. Equation (1) can then be written as

$$F = \dot{M}V_e \quad (2)$$

for all annular engines.

### 3.1.3 Throat Area

The nozzle throat cross-sectional area ( $A_t$ ) is a critical aspect of the chamber design. Although the nozzle throat area of an MCRI engine consists of three separate ring segments, it can be found in the same way as a conventional, bell shaped nozzle. For a given  $\dot{M}$ , throat pressure ( $P_t, psia$ ) and throat temperature ( $T_t, ^\circ R$ ), the total throat area ( $A_t, in^2$ ) is

$$A_t = \frac{\dot{M}}{P_t} \sqrt{\frac{RT_t}{\gamma g_c}} \quad (3)$$

where  $R$  is a specific gas constant ( $\frac{ftlb_f}{\circ R slug}$ ),  $\gamma$  is the specific heat ratio and  $g_c$  is the gravitational constant. The terms  $P_t$  and  $T_t$  are given by the following equations, respectively

$$P_t = P_c \left[ 1 + \frac{\gamma - 1}{2} \right]^{-\frac{\gamma}{\gamma - 1}} \quad (4)$$

$$T_t = T_c \left[ \frac{1}{1 + \frac{\gamma - 1}{2}} \right] \quad (5)$$

where  $P_c$  and  $T_c$  are the conditions in the combustion chamber [4, 5]. For a given inner throat radius ( $r_i$ ) and ring segment angle ( $\alpha$ ), the outer throat radius could be given by

$$r_o = \sqrt{\frac{360 A_t}{\alpha \pi} + r_i^2} \quad (6)$$

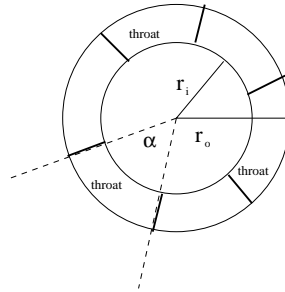


Figure 2: MCRI throat cross section

where  $r_i$ ,  $r_o$  and  $\alpha$  are as seen in Figure 2.

### 3.2 Sub-chamber Design

The combustion chamber section of an engine is where mixing of the propellants, ignition and burning takes place. In an MCRI engine, the combustion chamber is divided into multiple sub-chambers in order to allow two dimensional thrust vectoring. For this purpose, a minimum of three sub-chambers are needed. There is no maximum number of allowable sub-chambers, although each additional sub-chamber adds complexity to the engine, reducing overall engine reliability.

The MCRI test engine will have three sub-chambers. There are a number of characteristics one must consider when designing a combustion sub-chamber. The sub-chamber volume must be sufficiently large to allow complete combustion of the propellants. For MCRI engines, it is easiest to calculate the total chamber volume and then divide by the number of sub-chambers to determine the sub-chamber volume. By using the *characteristic length* ( $L^*$ ) of the chamber, one can get a very good approximation of the chamber volume ( $V_c$ ), where

$$V_c = L^* A_t. \quad (7)$$

The sub-chamber volume ( $V_{sc}$ ) is given by

$$V_{sc} = \frac{V_c}{n} \quad (8)$$

where  $n$  is the number of sub-chambers

The shape of the MCRI sub-chambers is important for several reasons. First, the overall length must be small enough to minimize losses due to high combustion velocities within the chamber [3]. In order to avoid combustion instabilities, the sub-chambers will be nearly cylindrical for the majority of the sub-chamber's length, lofting into a segmented annulus



at the throat [Figure 2]. A cylindrical shape also reduce hypertonic heat sections along the chamber wall that could cause material fatigue or failure. Machining limitations and the structural requirements of the chamber wall dictate a less than semi-circular inner chamber wall. Although this will cause some combustion instabilities, further study will be required to determine the full effects.

### 3.3 Nozzle Design

This section discusses the various possible shapes of the *spike*, or diverging nozzle section. Essentially, the job of the spike is to guide the expanding exhaust gasses downward in a smooth expansion pattern. In its most basic form, a spike is a simple cone. By adding a concave contour to the cone, the exhaust gasses expand quickly at first and are gradually directed downward, providing performance advantages similar to those seen in bell-shaped nozzles. When an annular engine is scaled up, the weight of a full spike is unacceptable. To reduce weight, the lower section of the spike is removed. This configuration is known as a *plug nozzle* [1] and is often accompanied by additional propellant flow through the base of the plug to compensate for otherwise poor aerodynamics. These three nozzle shapes are shown in Figure 3.

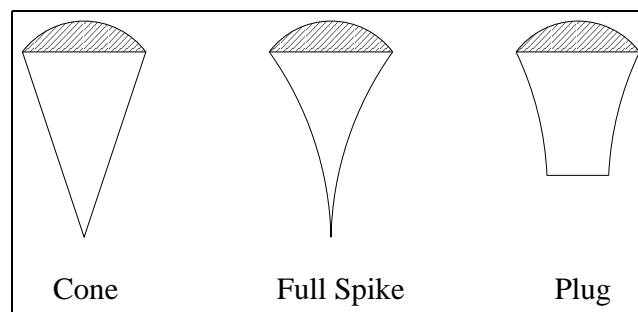


Figure 3: Annular Nozzle Shapes

The MCRI test engine will use a full spike nozzle for simplicity of design. Larger MCRI

engines would benefit from the reduced weight of a plug nozzle.

### 3.4 Engine Cooling

Engine cooling of MCRI engines is difficult for several reasons. First, MCRI engines have a lot of surface area to be cooled. For general purposes, heat flux ( $Q$ ) is given as

$$Q = qA \tag{9}$$

where  $q$  is the average heat transfer rate of the chamber ( $BTU/in^2/sec$ ) and  $A$  is the heat transfer area ( $in^2$ ), i.e., the chamber wall area. Heat transfer rate is dependent on the chosen materials, but the chamber wall area of an MCRI engine can be over three times that of a conventional rocket, requiring over three times the coolant capacity. In addition, MCRI engines are more likely to experience catastrophic heat buildup in the chamber dividing walls, where there is a concentrated heat flux in a small area, as well as in the inner chamber wall which cannot convect or radiate excess heat away.

There are several methods used for cooling rocket engines. The most commonly used method is *regenerative cooling* [1]. This method uses one or both of the propellants to cool the chamber wall. However, regenerative cooling only works with liquid propellants, which can absorb useful amounts of heat from the chamber wall. Because the MCRI test engine uses gaseous propellants, it must either use separate coolant, which is unnecessarily heavy for the flight engine, or use materials that can withstand the high heat flux. One method that could potentially provide considerable weight savings and high reliability involves depositing a laminate of high temperature, low thermal conductivity material such as a carbon-carbon (C-C) composite on the chamber wall. Such a material could withstand the relatively low combustion temperatures of  $GOX/GH_2$  propellants with minimal degradation and the low conductivity would not only lessen the heat flux through the chamber wall, but also allows

more efficient utilization of the combustion heat products. To provide additional cooling in the high heat flux areas of the outer chamber wall, this method could be coupled with *radiation cooling*. Radiation cooling uses a highly conductive material to radiate heat energy from the chamber wall [1].

### 3.5 Feed System

Nearly all liquid-propellant rocket engines use one of two types of propellant feed systems, often depending upon rocket size. Large rockets are generally pump-fed while smaller rockets ( $< 1000$  lbs thrust) are pressure-fed. The MCRI test engine uses pressurized gaseous propellants, and therefore will be pressure-fed. Typically, a pressure-fed system uses a pressurized tank of inert gas to pressurize the propellant tanks. However, the MCRI test engine uses pre-pressurized propellants and does not require any additional pressurization.

In an MCRI engine, the propellant feed system must be closely integrated with the Guidance Control Computer (GCC) in order to accomplish the individual chamber throttling required for thrust vectoring. The GCC will control the secondary regulators that determine the mass flow directly into the combustion chambers. By integrating a two-dimensional array of force sensors into the engine test stand, the thrust vector function ( $F = f(\dot{M})$ ) for the MCRI test engine will be determined. The GCC will use this function to determine the appropriate mass flow into each chamber for the necessary direction change. The primary regulators will be attached directly to the propellant tanks to minimize the need for heavy ultra-high pressure feed lines. In Figure 4, a simple integrated feed system is presented. Chamber pressure and temperature sensors may be added to monitor engine performance.

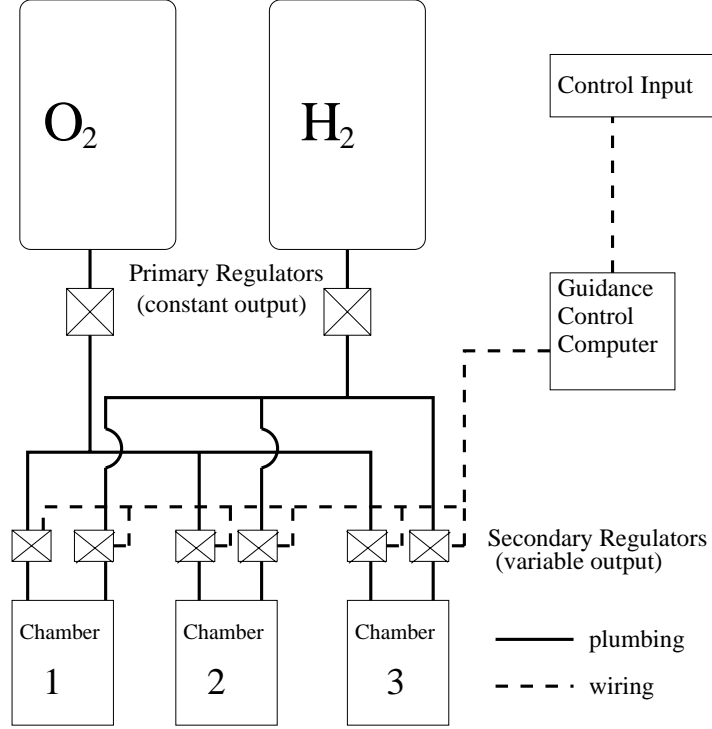


Figure 4: Schematic Diagram of Integrated Feed System

### 3.6 Thrust Vectoring

One of the most significant advantages of an MCRI engine is its ability to perform directional changes without mechanical devices directing the exhaust engine or the exhaust flow. This is important because mechanical devices are extremely heavy, adding to the vehicle weight, and extremely complicated, reducing the reliability of the overall engine. The MCRI engine performs thrust vectoring by differential throttling of the individual sub-chambers. Each sub-chamber is controlled individually by the Guidance Control Computer (GCC), which varies the mass flow into the chambers. A higher mass flow results in a higher chamber pressure and higher exit velocity (or a higher exhaust plume pressure relative to the other exhaust plumes). A difference in exhaust plume pressure bends the overall engine exhaust, effectively changing the momentum thrust vector.

### 3.6.1 Throttling

In a pressure fed system such as the MCRI test engine, throttling, or altering the thrust, is accomplished by regulating the propellant pressure into the chamber. This determines the mass flow ( $\dot{M}$ ) into the chamber. From equation (2), we recall that thrust for an annular engine is given by  $F = \dot{M}V_e$ . The exit velocity ( $V_e$ ) can be determined for a given nozzle, assuming  $\dot{M}$  is known, by the algorithm below.

The chamber pressure ( $P_c$ ) is determined by

$$P_c = \frac{\dot{M}C^*}{A_t} \quad (10)$$

where  $A_t$  is the throat area and  $C^*$  is the characteristic exhaust velocity for a given propellant combination, given by

$$C^* = \sqrt{\frac{1}{\gamma} \left( \frac{\gamma + 1}{2} \right)^{\frac{\gamma+1}{\gamma-1}} \frac{\bar{R}T_c}{M}} \quad (11)$$

where  $\gamma$  is the specific heat ratio,  $\bar{R}$  is the universal gas constant ( $1545.43 \frac{ft \cdot lb_f}{\circ R lb_m mole}$ ),  $T_c$  is the chamber temperature ( $\circ R$ ) and  $M$  is the molecular weight ( $\frac{lb_m}{mole}$ ) of the propellants. The exit Mach number ( $M_e$ ) is given by

$$M_e = \sqrt{\frac{2}{\gamma - 1} \left[ \left( \frac{P_c}{P_a} \right)^{\frac{\gamma-1}{\gamma}} - 1 \right]} \quad (12)$$

where  $P_a$  is the atmospheric pressure. In order to determine the actual exit velocity from the Mach number, one must know the local speed of sound ( $a_e$ , ft/sec), given by

$$a_e = \sqrt{\frac{\gamma \bar{R} T_e}{M}} \quad (13)$$

where  $T_e$  is the exit temperature ( $\circ R$ ), given by

$$T_e = \frac{T_c}{1 + \frac{\gamma-1}{2} M_e^2}. \quad (14)$$

From here, exit velocity is given by

$$V_e = a_e M_e. \quad (15)$$

The thrust is therefore entirely dependent upon the mass flow into the combustion chamber, assuming a constant mixture ratio. Figure 5 shows the output thrust of an MCRI test engine at throttle conditions between 50% and 105% of normal propellant mass flow. The relationship is “fairly” linear.

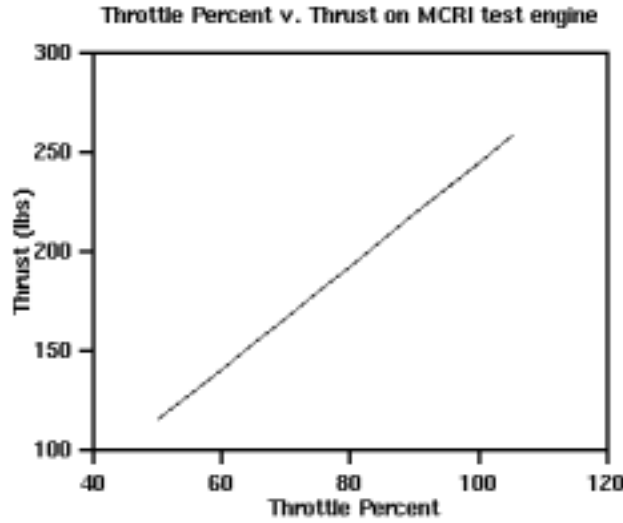


Figure 5: Thrust Curve Through Throttling of MCRI Test Engine

## 4 Future

Beginning this fall, the MCRI test engine will go through several test stages, concluding in hot fire tests of an actual engine. Given the proper resources, a finite element analysis

will be conducted prior to engine construction to determine the thermal requirements and mechanical stress of the engine. Further studies will be conducted to answer the following questions [Paul Eremenko<sup>2</sup>]:

- Will an MCRI engine's benefits overcome the fluid flow losses and frictional losses arising from its complicated geometry?
- How does the performance of an MCRI compare with other steerable, throttleable engines?
- Is there a market for MCRI engines?

## 4.1 Cold Flow Simulation

A cold flow (no combustion) MCRI engine using compressed air was constructed for the purpose of simulating the interaction of the exhaust plumes from the separate sub-chambers in order to answer the question of how significant an exhaust direction change can one achieve from differential throttling. Figure 6 shows the cold flow chamber assembly without the spike section. The cold flow MCRI has four cylindrical chambers between two polycarbonate



Figure 6: A Nearly Complete Cold Flow MCRI Engine

---

<sup>2</sup>Personal communication

flanges. The injector bulkhead (top flange) has NPT pipe fittings for compressed air injection. The nozzle bulkhead (bottom flange) has four 30° ring segment nozzles tapered at 10° on the outer diameter. A conical spike is attached on the bottom of the nozzle bulkhead. Figure 7 shows a section view of a cold flow MCRI engine.

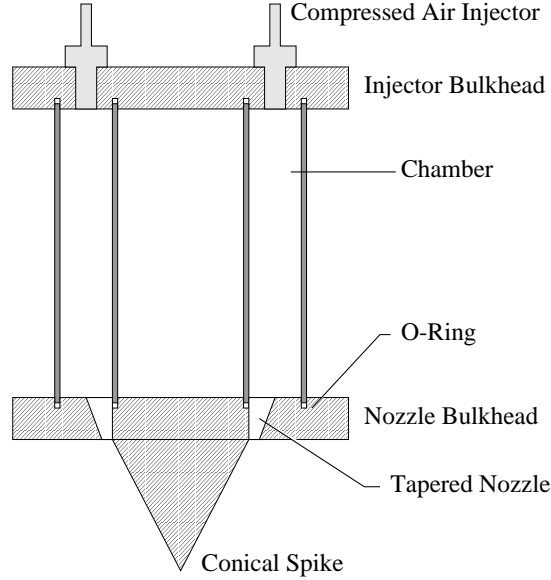


Figure 7: Diagram of a Cold Flow Compressed Air MCRI Engine

The cold flow MCRI engine will be used to simulate the exhaust flow at both constant thrust and differential throttling conditions. Individual pressure regulators will control the input pressure for each chamber. Pressures will range from 50 psi to 250 psi. The resulting exit velocities will range from Mach 1.5 to Mach 2.5 (see Equation (12)). A schlieren measurement will be used for flow visualization [6]. This method involves passing a white light through a thin slit, by a collimating mirror or lens and then through the flow field. The light is then focused by another mirror or lens and half of it is blocked by a knife edge. Density changes caused by supersonic shocks in the flow field refract the light away from the focal point. On the final image, these density changes will show up as either light or dark areas, depending on the direction of refraction.



## 4.2 Construction of Test Engine

Upon further funding, a fully functional test engine will be constructed to test engine performance. Custom components will be machined by a local machine shop from solid CAD drawings and off the shelf parts will be procured from various sources. Hot fire testing will be conducted at a site to be determined. The test stand will be incorporated with various sensors, including a force sensor array and a heat sensor. An example test stand with integrated force sensors is given in Figure (insert photo of CATS engine stand). The heat sensor will measure the exit temperature as a determinant of combustion efficiency. The output from the force sensor array will be used to determine the total thrust, as well as the thrust vector change corresponding to given differential throttle conditions.

All the data will be analyzed and used to refine the engine design for future MCRI engines.

## 5 Acknowledgments

I would like to thank my mentor, Col. John E. Keesee, for giving such incredible support and allowing me to pursue this idea, which I have been thinking about, on and off, for the past year. I would also like to thank my tutor Jenny Sendova for aiding me in any way I needed, my tutor group for being so enthusiastic and encouraging, Robbie Bryant, Adam De La Zerda, Balint Veto, Miro Jurišić and Paul Eremenko for helping in the revision process and Lisa Powell for providing the aforementioned contact. I am also grateful to Robert Lightfoot of Stennis Space Center for the information he provided and Don Weiner for machining assistance. Finally, I would like to thank the Research Science Institute and the Center for Excellence in Education, to which I am eternally grateful for giving me this fantastic opportunity.

## References

- [1] Huzel, D. K.; Huang, D. H.: Modern Engineering for Design of Liquid-Propellant Rocket Engines. *Progress in Astronautics and Aeronautics*: AIAA, 1992.
- [2] Davidian, Ken: The Aerospike Nozzle Frequently Asked Question List. *The Aerospike Nozzle Home Page*: 2001.
- [3] Sutton, George P.: Rocket Propulsion Elements, Sixth Edition. *John Wiley & Sons, Inc.*, 1992.
- [4] Hill, P. G.; Peterson, C. R.: Mechanics and Thermodynamics of Propulsion. *Addison-Wesley Publishing Company, Inc.*, 1965.
- [5] Krzycki, Leroy J.: How to Design, Build and Test Small Liquid-Fuel Rocket Engines. *Rocketlab*: 1967.
- [6] Lekki, John: Schlieren Measurement Technique. [http://www.lerc.nasa.gov/Other\\_Groups/OptInstr/schl.html](http://www.lerc.nasa.gov/Other_Groups/OptInstr/schl.html), July 20, 2002.

## A Appendix: MCRI Test Engine Specifications

---

---

Fuel .....	Gaseous Hydrogen ( $GH_2$ )
Oxidizer .....	Gaseous Oxygen ( $GOX$ )
Mixture Ratio O/F .....	4/1
Thrust .....	250 lb.s
Specific Impulse ( $I_{sp}$ ) .....	390 sec
Chamber Pressure $P_c$ .....	1000 psia
$M$ .....	10 kg/mol
$C^*$ .....	7836 ft/sec.
$T_c$ .....	5374 °R
Avg. Specific Gravity .....	0.28 g/cm <sup>3</sup>
$\gamma$ .....	1.26
Mass Flow $\dot{M}$ .....	0.0199 slugs/sec
$O_2$ Flow $\dot{M}_O$ .....	0.513 lb./sec
$H_2$ Flow $\dot{M}_F$ .....	0.128 lb./sec
Throat Temperature $T_t$ .....	4756 °R
Throat Pressure $P_t$ .....	553 psia
Gas Constant $R$ .....	154.5 (ftlb <sub>f</sub> /(slug°R))
Gravitational Constant $g_c$ .....	32.2 ft/sec <sup>2</sup>
Throat Area $A_t$ .....	0.156 in <sup>2</sup>
Characteristic Chamber Length $L^*$	25 in
Chamber Volume $V_c$ .....	160 in <sup>3</sup>
Sub-Chamber Volume $V_{sc}$ .....	53.3 in <sup>3</sup>

---

---